A Simple and Robust Adaptive Controller for Detuning Correction in Field-Oriented Induction Machines

Julio C. Moreira, *Member, IEEE*, Kam Tim Hung, Thomas A. Lipo, *Fellow, IEEE*, and Robert D. Lorenz, *Member, IEEE*

Abstract—**This work presents a novel adaptive controller for correcting the rotor time constant estimate used in the slip frequency calculator of indirect field-oriented controllers (IFOC's). The controller is novel in that it possess near digital deadbeat performance and simultaneously maintains its correctness down to zero speed. The robust controller dynamics are based on an operating-point form of digital deadbeat control. In this controller, an operating-point approximate inverse model relates changes in the machine parameters to deviation in the rotor flux components. This allows nearly exact, one-step (deadbeat) prediction of the correction necessary for the slip calculator gain. The correctness down to zero rotor speed is based on the determination of the rotor flux from an accurate air-gap flux estimate obtained from the third harmonic stator phase voltage component introduced by the saturation of the machine stator teeth. Moreover, a function relating the amplitude of the third harmonic air-gap flux component with the value of the magnetizing inductance allows correction of this machine parameter for different flux levels. The proposed adaptive controller is implemented in a digital signal processor, and the experimental results demonstrate its excellent performance for a wide range of rotor speeds, including locked rotor conditions.**

Introduction

TORQUE CONTROL of alternating current machines, including the induction motor, has drawn considerable attention in recent years. Both indirect and direct field orientation have been successfully established in theory and practice. In both control strategies, the stator current components responsible for the flux and torque production are decoupled via nonlinear state feedforward and feedback control loops. This achieves independent and linear control of torque and flux. Since its introduction in the early 1980's the direct field-orientation scheme has been regarded as less practical because of the sensors needed for obtaining information about the machine variables (e.g., search coils, coil taps, of Hall-effect sensors). In addition to increasing the total controller cost, these sensors often impose limitations on the machine operating range. By comparison, indirect field orientation has relatively simpler hardware and better overall performance especially at low frequencies. A basic implementation of an indirect field-orientation controller (IFOC) for an induction motor is shown in Fig. 1 in simplified block diagram form.

Typically, such controllers utilize machine parameter values (e.g., the the rotor time constant and the magnetizing inductance) to implement nonlinear feedforward calculation of the proper motor slip frequency $s\omega_e^*$ so that the conditions for rotor flux orientation (and, consequently, the decoupling of torque and flux) are achieved. As with all feedforward techniques, the decoupling accuracy is parameter dependent. When the rotor time constant T_r changes due to temperature or saturation level, the decoupling between the control variables is incorrect, and the control system operates in a detuned condition. Many methods have been proposed to solve this problem of detuning of the slip calculator, including identification, estimation, and adaptation [1]–[8].

In recent work by Hung and Lorenz in [9] and [10], a digital deadbeat adaptive controller was proposed and implemented. In that approach, an operating point approximate inverse model error function based on the rotor flux error was derived so that the deviation in the slip gain was predicted directly. The resulting adaptive controller can be viewed from a discrete time control point of view in which the feedback correction possesses a deadbeat characteristic allowing short, nearly one-step, convergence times. However, while such a controller removes the sensitivity to rotor parameters, it is sensitive to the stator resistance for low-speed operation. This limitation comes from the fact that the nonlinear rotor flux observer is based on the stator terminal voltages and currents.

In this paper, a new adaptive controller that combines the digital deadbeat adaptive controller presented in [10] is presented with an accurate flux sensing technique based on the saturation third harmonic component of the stator

Paper IPCSD 91-146, approved by the Industrial Drives Committee of the IEEE Industry Applications Society for presentation at the 1991 Industry Applications Society Annual Meeting, Dearborn, MI, September 28–October 4. This work was supported by the Wisconsin Electric Machines and Power Electronics Consortium (WEMPEC) in the Department of Electrical and Computer Engineering at the University of Wisconsin, Madison. Manuscript released for publication January 3, 1992.

J. C. Moreira is with the Research and Engineering Center, Whirlpool Corporation, Benton Harbor, MI 49022.

K. T. Hung, T. A. Lipo, and R. D. Lorenz are with the Department of Electrical and Computer Engineering, University of Wisconsin, Madison, WI 53706-1691.

IEEE Log Number 9203288.

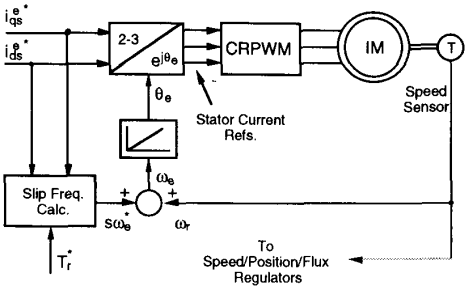

Fig. 1. Implementation of an indirect field-orientation controller (IFOC) for an induction motor.

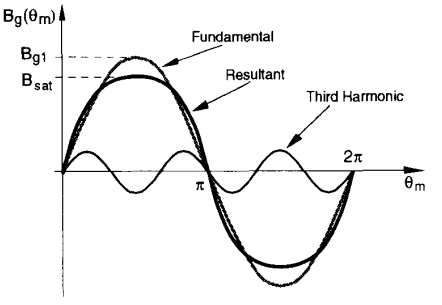

Fig. 2. Actual air-gap flux density distribution for an induction machine operating at rated voltage (heavy line). Its fundamental and third harmonic components are also shown.

voltages as introduced in [11] and [12]. The resulting controller combines the control robustness and superior performance of the deadbeat adaptive controller with the accuracy of direct flux sensing. This combination is shown to be practically independent of machine parameters and to exhibit superior performance compared with previous detuning correction solutions. The experimental results demonstrate the robustness of the controller over a wide range of rotor speed, including zero speed, for which the slip calculator gain can still be tuned to its correct value.

The following sections describe the methodology of estimating the rotor flux from the stator third harmonic voltage, the methodology for deadbeat disturbance rejection control design, the derivation of an approximate inverse deadbeat control model for the induction motor, the implementation of the deadbeat adaptive controller, and the experimental results on an induction motor field-oriented drive system.

Estimation of Rotor Flux Via The Saturation Third Harmonic

As described in detail in [11] and [12], induction machines are designed to work in the saturation region of the *B-H* characteristic of their magnetic core material. As a consequence of saturation, the teeth with the highest flux density will saturate, and the air-gap flux distribution will assume a flattened sinusoidal form with peak value B_{sat} as shown in Fig. 2.

The flattening of the sine wave of the air-gap flux density is produced by the nonlinear magnetic *B-H* curve of the steel. This flattening causes a third harmonic flux component. Consequently, the third harmonic of the air-gap flux links the stator winding and induces a third harmonic component in each one of the stator phase voltages that are in phase, forming a zero sequence set of voltages. If the stator phases are star connected, no third harmonic currents will circulate in the stator side, and no third harmonic voltage drop will exist in the stator impedance. Therefore, the stator third harmonic voltage will always be in phase with the third harmonic voltage component of the air-gap voltage regarding the load condition of the induction machine. This fact is especially important when locating the position of the fundamental component of the air-gap flux with respect to the stator current, as will be discussed later.

When the three stator phase voltages are summed, the fundamental and characteristic harmonics are canceled, and the resultant waveform contains mainly a third harmonic component and a high-frequency component due to the rotor slots. This resultant third harmonic voltage term v_{s3} can be integrated so that the resulting flux signal λ_3 has an amplitude that can be related to the fundamental amplitude of the air-gap flux λ_{am} or λ_m via a saturation function f_λ, as in (1). This saturation function is easily obtained experimentally from the results of a conventional no-load test.

$$|\lambda_{am}| = f_\lambda(|\lambda_3|). \tag{1}$$

The relative position of the fundamental component of the air gap flux with respect to the stator current is obtained by measuring the phase displacement between two fixed points in the third harmonic flux and the line current. Fig. 3 shows this phase displacement γ_{im} between the maximum values for the fundamental components of current and air-gap flux.

The fundamental and third harmonic components of the air-gap flux and the stator current are depicted in Fig. 4 in a synchronously rotating reference frame representation for a condition of field orientation.

It is clear from this vector arrangement that the air-gap flux, after having its amplitude $|\lambda_m|$ and its relative position γ_{im} estimated from the third harmonic flux and current signals, can be resolved into its d and q components according to

$$\lambda^e_{dm} = -|\lambda^e_m| \sin(\theta_{is} + \gamma_{im}) = -f_\lambda(|\lambda^e_3|) \sin(\theta_{is} + \gamma_{im}) \tag{2}$$

$$\lambda^e_{qm} = |\lambda^e_m| \cos(\theta_{is} + \gamma_{im}) = f_\lambda(|\lambda^e_3|) \cos(\theta_{is} + \gamma_{im}) \tag{3}$$

with θ_{is} computed from the reference values for the stator currents i^{e*}_{qs} and i^{e*}_{ds} as indicated by (4)

$$\theta_{is} = -\tan^{-1}\left(\frac{i^{e*}_{ds}}{i^{e*}_{qs}}\right). \tag{4}$$

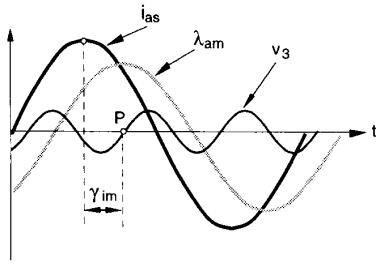

Fig. 3. Fundamental components of stator line current i_{as}, fundamental air gap flux (λ_{am}), and third harmonic voltage (V_3) components. γ_{im} is the phase displacement between the stator current and air-gap flux.

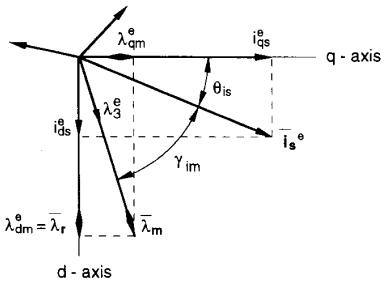

Fig. 4. Stator current, air-gap flux, and third harmonic flux vectors in the synchronous reference frame for a rotor flux orientation condition.

The rotor flux components can be derived as a function of the air-gap flux and stator current components as in the following equations:

$$\lambda^e_{qr} = \frac{\hat{L}_r}{\hat{L}_m}\lambda^e_{qm} - \hat{L}_{lr} i^e_{qs} \tag{5}$$

$$\lambda^e_{dr} = \frac{\hat{L}_r}{\hat{L}_m}\lambda^e_{dm} - \hat{L}_{lr} i^e_{ds} \tag{6}$$

where $\hat{L}_r$, $\hat{L}_m$, and $\hat{L}_{lr}$, represent, respectively, the estimates for the rotor, magnetizing, and rotor leakage inductances. Although dependent on machine parameters, the rotor flux can be obtained with reasonable accuracy since the rotor leakage inductance $\hat{L}_{lr}$ and the ratio $\hat{L}_r/\hat{L}_m$ are only moderately dependent on the saturation level. Changes in the magnetizing inductance with flux or load levels can be corrected via a function relating the actual value of the magnetizing inductance with the magnitude of the third harmonic flux component, which is readily obtained from the function relating the air-gap flux and third harmonic flux amplitudes described by (1). This, combined with the fact that the rotor leakage inductance can be assumed to be practically constant for normal operating conditions, guarantees a very good robustness for the estimation of the rotor flux for a wide speed range.

With the fundamental of the air-gap flux linkage located from the third harmonic voltage signal, a direct air-gap field orientation strategy can be implemented as a first intuitive approach. In this control scheme, the air-gap flux is aligned with the d axis of the d-q plane with the stator current components i_{qs} and i_{ds} being, respectively, the command variables for the induction motor torque and flux. Unfortunately, this type of field-orientation scheme does not allow a complete decoupling between the commanded variables that can be achieved only by the introduction of a decoupling network. This decoupling network, however, brings the disadvantage to the system being dependent on sensitive machine parameters as well as by adding complexity to the control algorithm. Another potential problem of this type of controller relates to the static stability of the drive, which will present a limited pull-out torque if a current command is used for the flux control [13].

Deadbeat Disturbance Rejection Control Design

The basic principles of deadbeat control are usually understood as a closed-loop discrete time system that achieves its final value after a finite number of sample periods. Let us assume, for the generic z-transform discrete-time closed-loop control shown in Fig. 5, a desirable transfer function given by

$$\frac{\phi}{\phi^*} = z^{-1} \tag{7}$$

or a difference equation model

$$\phi(k) = \phi^*(k-1). \tag{8}$$

A controller $G_c(z)$ can be designed for a general closed-loop system with a disturbance input as that shown in Fig. 5 so that (7) applies.

For this closed-loop system, the command response is

$$\frac{\phi}{\phi^*} = \frac{Gc(z)Gp(z)}{1 + Gc(z)Gp(z)}. \tag{9}$$

Combining (7) and (8) yields the required deadbeat controller

$$G_c(z) = G_p(z)^{-1}\frac{z^{-1}}{1 - z^{-1}}. \tag{10}$$

This deadbeat command response controller consists of the following two parts:

$G_p(z)^{-1}$ inverse model of the process

$\dfrac{z^{-1}}{1 - z^{-1}}$ one-step delayed integration process.

It is important to note that the deadbeat controller uses the following:

- The inverse model of the process to calculate the input U_c required to produce the desired output ϕ
- the integration process to hold that value of U_c to maintain the desired output ϕ.

This same block diagram can be reformulated, as shown in Fig. 6, to show a disturbance input U_d and the closed-loop controller's disturbance correction response U_c.

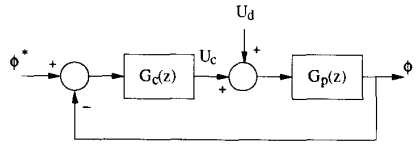

Fig. 5. z-transform, discrete-time, closed-loop control system with command ϕ^* and a disturbance input U_d.

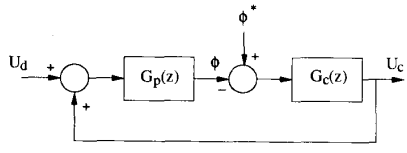

Fig. 6. z-transform, discrete-time, closed-loop control system with disturbance input U_d and a command ϕ^*.

This form shows how the closed-loop control system can be thought of as a means of producing a correction response to a disturbance input. The best possible correction response is deadbeat, just as it was for the command-driven form. In this case, that would imply a difference equation model

$$U_c(k) = U_d(k-1). \tag{11}$$

This closed-loop transfer function is the same as (8), i.e.

$$\frac{U_c}{U_d} = \frac{G_c(z)G_p(z)}{1 + G_c(z)G_p(z)}. \tag{12}$$

Thus, for deadbeat disturbance correction response, the controller is exactly the same as (10).

If this controller (10) is applied, the output response to a disturbance would be

$$\phi(z)|_{\text{dist. resp.}} = U_d \cdot G_p(z) \cdot (1 - z^{-1}). \tag{13}$$

If the open-loop disturbance response $U_d(z) \cdot G_p(z)$ varies slowly, then after one sample period, the net effect is nearly cancelled by the subtraction action

$$\phi(k)|_{\text{dist. resp.}} = G_p \cdot U_d(k) - G_p \cdot U_d(k-1). \tag{14}$$

Thus, this form of deadbeat controller can virtually eliminated the error response caused by the disturbance.

This simplified model can now be replaced by a slip gain form of the field-oriented controller as shown in Fig. 7.

This model shows how the unknown change in rotor resistance Δr_r produces a slip gain disturbance ΔK_s. This slip gain disturbance also produces a change in rotor flux $\Delta\lambda_r$ from the commanded values of

$$\lambda_{dr} = \lambda_{dr}^*, \lambda_{qr}^* = 0. \tag{15}$$

Since this model is analogous to the general model used for deadbeat design analysis, it should be apparent that

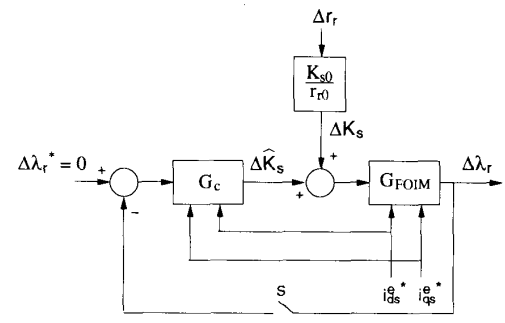

Fig. 7. Slip gain error driven, discrete time, closed-loop control system with disturbance input Δr_r (FOIM denotes field-oriented induction motor).

for deadbeat disturbance rejection, i.e.

$$\frac{\Delta\hat{K}_s}{\Delta K_s} = z^{-1} \tag{16}$$

the corresponding controller would be

$$G_c(z) = G_{\text{FOIM}}(z)^{-1} \frac{z^{-1}}{1 - z^{-1}}. \tag{17}$$

This result confirms that deadbeat disturbance rejection response properties for slip gain errors can be obtained if an inverse model of the field-oriented induction machine (FOIM) can be formed and used in the controller. Because the machine model is nonlinear, the inverse model will be a linearized operating point model. Thus, the controller will produce "near deadbeat" response. The derivation of this inverse model is the subject of the following section.

Approximate Inverse, Deadbeat Controller Model For The Field-Oriented Induction Machine

The basic principle of this controller, as discussed in [9] and [10], is to measure the rotor flux error for use as a feedback signal to the deadbeat controller, which computes the needed slip frequency correction $\Delta\hat{K}_S$. The rotor flux error relationship to the slip gain error when detuning occurs is the key point in the implementation of the deadbeat adaptive controller. The two rotor flux components are affected by any amount of detuning due to changes in the machine parameters, as the following analysis demonstrates.

The q-axis rotor voltage for a squirrel-cage induction motor can be written as

$$0 = r_r i_{qr}^e + p\lambda_{qr}^e + \omega_s \lambda_{dr}^e. \tag{18}$$

Because the detuning is mainly caused by changes in the rotor resistance that occur at a slow rate, it is a reasonable approximation to assume that the term $p\lambda_{qr}^e$ is close to zero. Hence, (18) above can be rewritten as

$$0 = r_r i_{qr}^e + \omega_s \lambda_{dr}^e. \tag{19}$$

The q-axis rotor flux for a nonsaturated machine is given by

$$\lambda_{qr}^{e} = L_m i_{qs}^{e} + L_r i_{qr}^{e}. \tag{20}$$

and solution for the slip frequency ω_s from (19) after substituting i_{qr}^{e} from (20) yields

$$\omega_s = \frac{L_m}{T_r} i_{qs}^{e} \lambda_{dr}^{e-1} - \frac{1}{T_r} \lambda_{qr}^{e} \lambda_{dr}^{e-1} = m i_{qs}^{e} \lambda_{dr}^{e-1} - n \lambda_{qr}^{e} \lambda_{dr}^{e-1}. \tag{21}$$

With the machine operating under field orientation, the commanded slip frequency $\omega_s^* = \omega_s$ and the estimates $\hat{m}$ and $\hat{n}$ coincide with the actual values for m and n in the equation above, as is shown by

$$\omega_s^* = \hat{m} i_{qs}^{e^*} \lambda_{dr}^{e^{*-1}} \tag{22}$$

where the q-axis component of the rotor flux is zero.

When a detuning condition occurs, an error in the parameter estimates (as well as in the rotor flux components) appears such that the slip frequency given by (21) becomes

$$\omega_s = (\hat{m} + \Delta m)(\lambda_{dr}^{e^{*-1}} - \Delta\lambda_{dr}^{e-1}) i_{qs}^{e} - (\hat{n} + \Delta n)(\lambda_{qr}^{e^*} + \Delta\lambda_{qr}^{e})(\lambda_{dr}^{e^{*-1}} - \Delta\lambda_{dr}^{e-1}) \tag{23}$$

which, after identifying the terms that correspond to the definition for ω_s, reduces to

$$0 = \Delta m \lambda_{dr}^{e^{*-1}} i_{qs}^{e} - \hat{m}\Delta\lambda_{dr}^{e-1} i_{qs}^{e} - \hat{n}\lambda_{dr}^{e^{*-1}}\Delta\lambda_{qr}^{e}. \tag{24}$$

Alternatively, the expression for Δm above can be expressed in terms of the actual d-axis rotor flux, instead of its reference value, as

$$\frac{\Delta m}{\hat{m}} = \frac{\Delta\lambda_{dr}^{e}}{\lambda_{dr}^{e}} + \frac{\Delta\lambda_{qr}^{e}}{\hat{L}_m i_{qs}^{e^*}}. \tag{25}$$

As a result, the deviation in the parameter estimation represented by Δm is readily computed as a function of the error in the d and q components of the rotor flux. This error is used by the controller algorithm to compute the necessary change in the slip gain commanded to the slip frequency calculator. When Δm is added to the estimate $\hat{m}$, (22) yields

$$\omega_s^* = (\hat{m} + \Delta m) i_{qs}^{e^*} \lambda_{dr}^{e^{*-1}} = (K_s^* + \Delta K_s) i_{qs}^{e^*} \tag{26}$$

where the symbol K_s^* is the rated slip gain computed from (27), and ΔK_s is its variation obtained from (25)

$$K_s^* = \hat{m} \lambda_{dr}^{e^{*-1}} = \frac{\hat{L}_m}{T_r^*} \frac{1}{\lambda_{dr}^{e^*}}. \tag{27}$$

Implementation of a Nearly Deadbeat Adaptive Controller

Fig. 8 illustrates the experimental IFOC drive system that has been implemented. Both the adaptive and the field-orientation control algorithms are implemented using a digital signal processor with two look-up tables containing the nonlinear functions f_λ and f_{Lm}. The sample rate for the deadbeat control loop was 10 Hz, which was deemed sufficient for rotor resistance thermal dynamics.

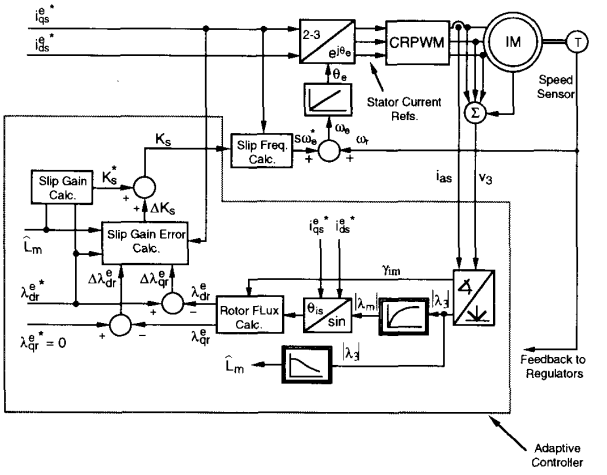

Fig. 8. Implementation of the nearly deadbeat adaptive IFOC controller for the rotor time constant with the magnetizing inductance estimate based on the amplitude of the third harmonic voltage signal.

Experimental Results

Fig. 9 shows the third harmonic stator voltage signal obtained from the summation of the three-phase voltages for operation at no-load and synchronous frequency around 30 Hz. A current-regulated PWM inverter is used to supply the induction machine. A wound rotor induction machine described in Table I is used with an external three-phase rehostat to simulate changes in the rotor resistance. In using such a scheme, we have in mind that second-order phenomena like saturation of the rotor leakage inductance and skin effect have their influence minimized. The changes in these parameters are not the focus of our study at this point.

Fig. 9(a) shows that third harmonic voltage and one of the line currents. The switching frequency component in the third harmonic voltage can be easily eliminated by a low-pass filter (LPF). Another LPF is used for the current so that the phase displacement between the current and third harmonic voltage is kept at its original value. It can be verified that the two points shown in the figure correspond to the maximum values for the air-gap flux and current since the zero crossing for the voltage waveform corresponds to a maximum value for the flux.

As expected, for a no-load condition, the phase shift between these two points, which represents the phase shift between the fundamental components of air-gap flux and stator mmf, is very small since the mechanical output power is developed only to overcome the windage and friction losses. As the machine is loaded, this phase shift increases to respond to the torque required by the load.

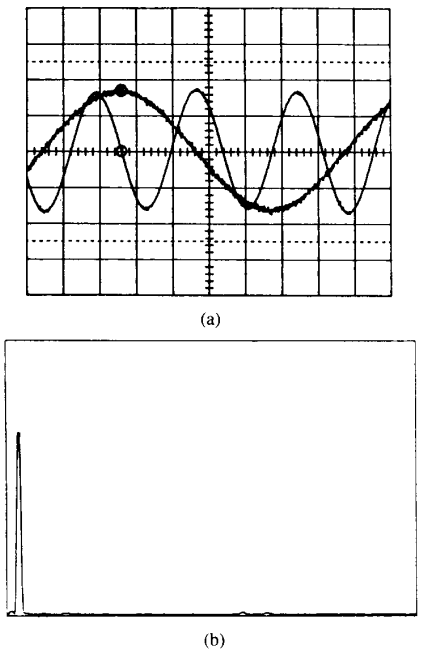

Fig. 9. Experimental results obtained for the test motor: (a) Line current (1 A/div) and stator third harmonic voltage (5 V/div), Hor: 4 ms/div; (b) third harmonic voltage spectrum (full scale of 10 V-rms), freq: 0–2000 Hz full scale.

TABLE I
TEST INDUCTION MOTOR PARAMETERS

Quantity	Symbol	Value
Line Voltage	Vl	200 V rms
Output power	P_o	1/3 hp
Speed	ω_r	1725 r/min
Poles	P	4
Frame	-	56T60
Stator resistance	r_s	7.15 Ω
Rotor resistance	r_r	6.0 Ω
Stator leakage reactance	X_{ls}	5.14 Ω
Rotor leakage reactance	X_{lr}	3.23 Ω
Unsaturated mag. reactance	X_m	100.65 Ω
Rotor inertia	J_m	0.022 Kg-m^2
Number of rotor slots	n_r	33
Number of stator slots	n_s	36
Air-gap length	g_o	1.28 mm
Rotor skew	-	1 slot
Stator pole pitch	τ_s	7/9
Rotor stack length	l_m	46.18 mm

As mentioned before, the high-frequency components in the third harmonic are easily eliminated by a simple filter, making this signal convenient for analog or digital processing.

The integration of the third harmonic voltage signal is performed by a digitally implemented LPF. The filter cut-off frequency is set to a low value (around 0.1 Hz) in order to minimize the integration error when operating with low frequencies as in the case of a locked rotor condition.

The spectrum contents for the third harmonic signal is analyzed and shown in Fig. 9(b). As predicted, after the summation of the three phase voltages, all the polyphase components are eliminated, and the third harmonic is clearly the dominant component at the lower side of the frequency spectrum. The PWM inverter utilized for these measurements has a variable switching frequency (3–5 kHz), which may have an amplitude comparable with the third harmonic signal and hence needs, to be filtered. The nearly deadbeat controller of Fig. 8 was implemented in the laboratory, and Figs. 10–12 show some of the experimental results.

Fig. 10 shows (from top to bottom) the evolution of the slip gain, the q-axis component of the rotor flux, the d-axis component of the rotor flux, and mechanical speed. This data was taken for a test motor coupled to a dynamometer running at rated torque and flux. The rotor resistance was doubled initially and then returned to the nominal value (both step changes). The correction for the slip gain is very fast, taking less than 2 s for the controller to command the right slip gain. Note that the response of the system for the two changes of the rotor resistance is slightly different. This is a consequence of the nonlinearity, which is not exactly modeled in the "nearly" deadbeat controller.

To investigate the third harmonic sensing capability at low flux levels, the same test described in Fig. 10 was carried out with a flux command of 50% of the rated value with the results shown in Fig. 11. These results demonstrate that even at reduced levels of saturation, the third harmonic signal remains useful for estimating the rotor flux.

Fig. 12 shows the nearly ideal performance of the experimental controller under locked rotor conditions at rated torque and rated flux values. The results show that even at zero speed (locked rotor), the nearly deadbeat controller achieves excellent dynamic performance and that the third harmonic flux estimation makes the tuning correct and independent of the stator impedance at low speeds. The same variables shown in the previous figure are shown again in this figure for the same amount of change in the rotor resistance as for the case above. The system has an excellent response and is not matched by previous reported controllers operating at these same conditions. Note that the error generated in the rotor flux components and the type of response are essentially the same as that for the case in Figs. 10 and 11.

CONCLUSIONS

A simple and robust method for correcting the rotor time constant in indirect field-oriented control of induction machines has been presented. The adaptive controller proposed is based on a nearly deadbeat structure that has the objective of eliminating rotor flux disturbances by commanding the correct slip gain as predicted from an approximate inverse model of the machine.

In addition to excellent dynamics, the nearly deadbeat controller is made accurate by the measurement of the

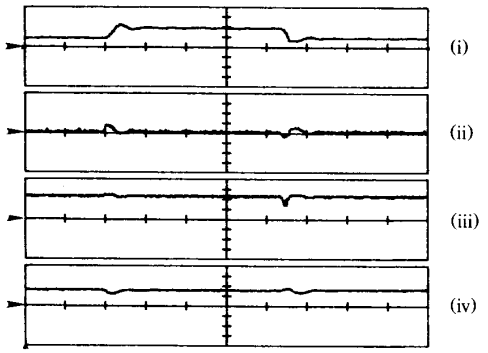

Fig. 10. Experimental results for the nearly deadbeat adaptive controller implemented in an IFOC driving the test motor at rated torque and rated flux commands. The rotor resistance is doubled at 4 s (step change) and returned to its nominal value after about 9 s (step change). From top to bottom: (Hor: 2 s/div): (i) Slip gain (10 Hz/A/div); (ii) q-axis component of the rotor flux (0.2 V.s/div); (iii) d-axis component of the rotor flux (0.2 V.s/div); (iv) mechanical speed (300 r/min/div).

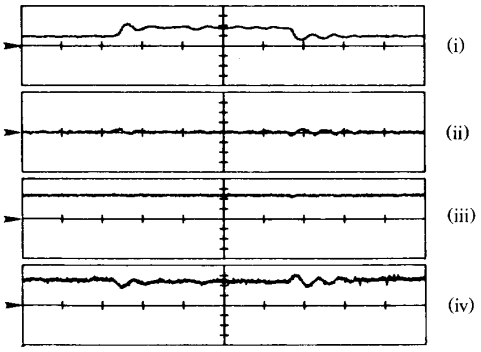

Fig. 11. Experimental results for the nearly deadbeat adaptive controller implemented in an IFOC driving the test motor at rated torque and 50% flux commands. The rotor resistance is doubled at 4 s (step change) and returned to its nominal value after about 9 s (step change). From top to bottom: (Hor: 2 s/div): (i) Slip gain (10 Hz/A/div); (ii) q-axis component of the rotor flux (0.2 V.s/div); (iii) d-axis component of the rotor flux (0.2 V.s/div); (iv) mechanical speed (300 r/min/div).

air-gap flux from the third harmonic component of stator voltage and estimation of the rotor flux.

This method also requires knowledge of the machine magnetizing inductance, which cannot be considered a constant under practical circumstances. Therefore, a correction strategy for changes in the magnetizing inductance with flux level is implemented in the controller. This correction strategy is based on a function relating the value of the inductance with the amplitude of the third harmonic flux signal. Consequently, the controller becomes independent of variations of the magnetizing inductance.

The experimental implementation of the nearly deadbeat controller has used a Motorola 56001 digital signal processor. However, the DSP speed was not needed for this loop since a 10-Hz sample rate was used for the deadbeat controller. This controller was part of a DSP-based indirect field-oriented drive used with a wound

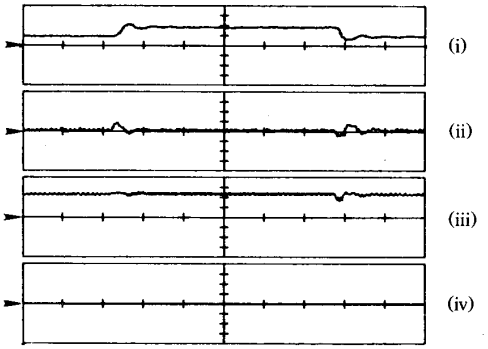

Fig. 12. Experimental results for the nearly deadbeat controller implemented as part of an IFOC driving the test motor at rated torque and rated flux commands at zero speed. The rotor resistance is doubled at a time approximately 4 s (step change) from the beginning of the trace and returned to its nominal value after about 12 s (step change). From top to bottom: (Hor: 2 s/div): (i) Slip gain (10 Hz/A/div); (ii) q-axis component of the rotor flux (0.2 V.s/div); (iii) d-axis component of the rotor flux (0.2 V.s/div); (iv) mechanical speed (zero r/min).

rotor induction motor. The system clearly has excellent response for speeds ranging from *zero* to twice the rated value, which is unmatched by previous reported controllers operating under the same conditions.

REFERENCES

[1] L. J. Garces, "Parameter adaption for the speed-controlled static ac drive with a squirrel-cage induction motor," *IEEE Trans. Industry Applications*, vol. IA-16, no. 2, pp. 173–178, Mar./Apr. 1980.

[2] T. Matsuo and T. A. Lipo, "A rotor parameter identification scheme for vector-controlled induction motor drives," *IEEE Trans. Industry Applications*, vol. IA-21, no. 4, pp. 624–632, May/June 1985.

[3] K. B. Nordin, D. W. Novotny, and D. S. Zinger, "The influence of motor parameter deviations in feedforward field orientation drive systems," *IEEE Trans. Industry Applications*, vol. IA-21, no. 4, pp. 1009–1015, July/August 1985.

[4] L. C. Zai and T. A. Lipo, "An extended Kalman filter approach to rotor time constant measurement in PWM induction motor drives," in *Proc. 1987 IEEE Industry Applications Soc. Ann. Mtg.*, Oct. 1987.

[5] H. Sugimoto and S. Tamai, "Secondary resistance identification of an induction-motor applied model reference adaptive system and its characteristics," *IEEE Trans. Industry Applications*, vol. IA-23, no. 2, pp, 296–303, Mar./Apr. 1987.

[6] C. Wang, D. W. Novotny, and T. A. Lipo, "An automated rotor time constant measurement system for indirect field-oriented drives," *IEEE Trans. Industry Applications*, vol. 24, no. 1, pp. 151–159, Jan./Feb. 1988.

[7] R. D. Lorenz and D. B. Lawson, "A simplified approach to continuous on-line tuning of field oriented induction machine drives," in *Proc. 1988 IEEE Industry Applications Soc. Ann. Mtg.*, 1988, pp. 444–449.

[8] T. M. Rowan, R. J. Kerkman, and D. Leggate "A simple on-line adaption for indirect field orientation of an induction machine," in *Proc. 1989 IEEE Industry Applications Soc. Ann. Mtg.*, 1989, pp. 579–587.

[9] K. T. Hung and R. D. Lorenz, "A rotor flux error-based, adaptive tuning approach for feedforward field oriented induction machine drives," in *Proc. 1990 IEEE Industry Applications Soc. Ann. Mtg.*, Oct. 1990.

[10] K. T. Hung, "A slip gain error model-based correction scheme of near-deadbeat response for indirect field orientation," *Master thesis*, Univ. of Wisconsin-Madison, 1990.

[11] J. C. Moreira, "A study of saturation harmonics with applications in induction motor drives," Ph.D. thesis, Univ. of Wisconsin-Madison, 1990.

[12] J. C. Moreira and T. A. Lipo, " A new method for rotor time constant tuning in indirect field oriented control," in *Proc. 1990 IEEE Power Electron. Spec. Conf.* (San Antonio, TX), June 10–15.

[13] R. De Doncker, "Synthesis and digital implementation of adaptive field orientation controllers for induction machines with air gap flux control and deep bar compensation," Ph.D. disseration, Katholieke Univ. Leuven, Belgium, 1986.

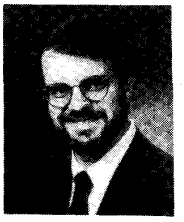

Julio C. Moreira (S'81–M'90) was born in Sao Paulo, Brazil. He received the B.E.E. and M.E.E. degrees in 1979 and 1983, respectively, from the State University of Campinas (UNICAMP). He received the Ph.D. degree in electrical engineering from the University of Wisconsin, Madison, in 1990.

He worked as an Engineer and later as a Vice Coordinator of the Electric Drive Systems Research Laboratory at UNICAMP from 1980 to 1985. In 1981, he became a Researcher and an Assistant Professor at that same institution, teaching courses in electrical machines, power electronics, and controls. His research activities included the development of dc and ac motor drives for an electric vehicle. He also served as a consultant in the areas of electric drive systems and switched power supplies. He later joined the Whirlpool Corporate Research and Engineering Center, Benton Harbor, MI, where he is involved with research in the areas of power electronics, electric drive systems, controls, and motor design.

Dr. Moreira is a member of ETA NOΣ, IAS, PES, and IES.

Kam Tim Hung was born in Hong Kong. He received the B.S. degree in electrical engineering from the Louisiana State University, Baton Rouge, in 1987 and the M.S. degree in electrical engineering from the University of Wisconsin-Madison in 1990.

Presently, he works in Hong Kong as a computer and software designer for electric motor drive systems.

Mr. Hung is a member of Phi Kappa Phi and Tau Beta Pi.

Thomas A. Lipo (M'64–SM'71–F'87) received the B.E.E. and M.S.E.E. degrees from Marquette University, Milwaukee, WI, in 1962 and 1964, respectively, and the Ph.D. degree in electrical engineering from the University of Wisconsin in 1968. He was an NRC Postdoctoral Fellow at the University of Manchester Institute of Science and Technology, Manchester, England, from 1968 to 1969.

From 1969 to 1979, he was an Electrical Engineer in the Power Electronics Laboratory of Corporate Research and Development of the General Electric Company, Schenectady, NY. He became Professor of Electrical Engineering at Purdue University, Lafayette, IN, in 1979 and later joined the University of Wisconsin, Madison, in the same capacity. He has been involved in the research of power electronics and ac drives for over 25 years.

Dr. Lipo has received 11 IEEE prize paper awards including corecipient of the Best Paper Award in IEEE TRANSACTIONS ON INDUSTRY APPLICATIONS for 1984. In 1986, he received the Outstanding Achievement Award from the IEEE Industry Applications Society for his contributions to the field of ac drives.

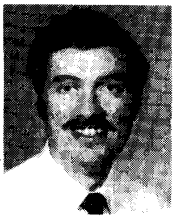

Robert D. Lorenz (S'83–M'84) received the B.S., M.S., and Ph.D. degrees, all in mechanical engineering (electro-mechanics and control specialty), from the University of Wisconsin, Madison, in 1969, 1970, and 1984, respectively.

Since 1984, he has been a member of the faculty of the University of Wisconsin, Madison, where he is an Associate Professor of Mechanical Engineering and Affiliate Associate Professor of Electrical and Computer Engineering. In this position, he acts as Associate Director of the Wisconsin Electric Machines and Power Electronics Consortium and as Co-Director of the Advanced Automation and Robotics Consortium. He was a Visiting Research Professor in the Electrical Drives Group of the Catholic University of Leuven, Belgium, and in the Electrical Drive Institute of the Technical University of Aachen, West Germany, in the Summers of 1989 and 1987, respectively. In 1969-70, he did his Master thesis research at the Technical University of Aachen, West Germany. From 1972 to 1982, he was a member of the research staff at the Gleason Works in Rochester, NY. His current research interests include optical and electromagnetic sensor technologies, real-time digital signal processing techniques, electromagnetic actuator design and control, and ac drive and high-precision machine control technologies.

Dr. Lorenz is a member of the IAS Industrial Drives Committee, the Machine Tools, Robotics, and Factory Automation Committee, and the Industrial Control Committee. He is an active consultant to many organizations and is a Registered Professional Engineer in the States of New York and Wisconsin. He is a member of the ASME, and ISA, and the SPIE.